

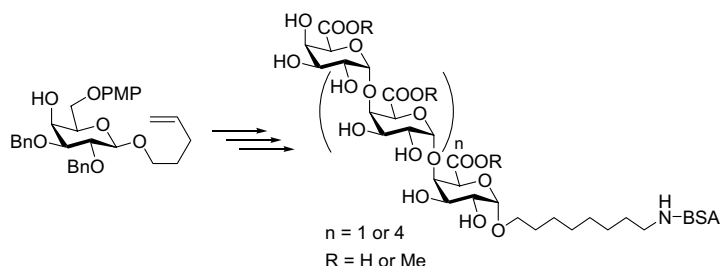
Contents

FULL PAPERS

Synthesis of oligogalacturonates conjugated to BSA

pp 2159–2169

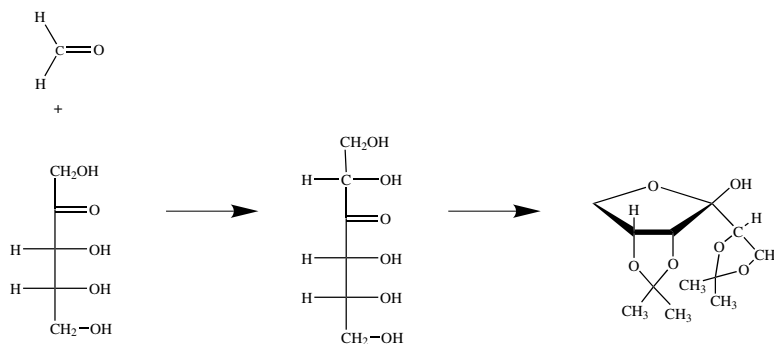
Mads H. Clausen and Robert Madsen*



Formation of 3-hexuloses in aldol reactions, analysis of the products as their *O*-isopropylidene derivatives by GC–MS

pp 2171–2176

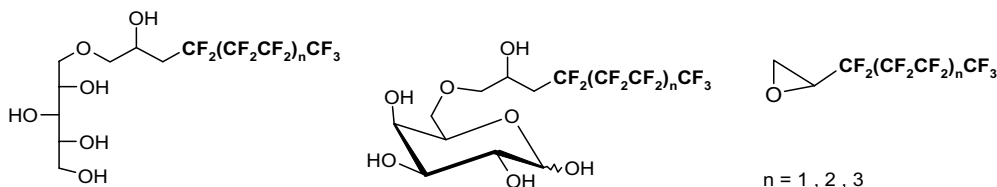
Dag Ekeberg and Svein Morgenlie*



Novel perfluoroalkylated derivatives of D-galactopyranose and xylitol for biomedical uses. Hemocompatibility and effect on perfluorocarbon emulsions

pp 2177–2185

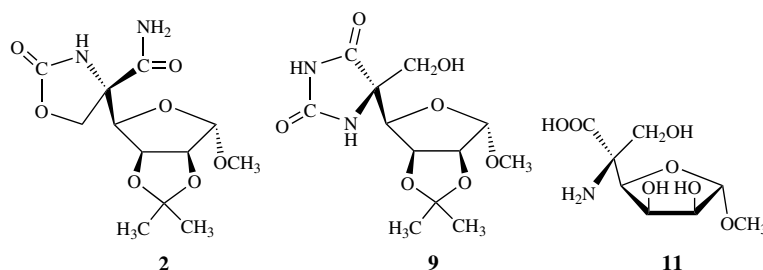
Vladimír Církva, Radek Polák, Oldřich Paleta,* Karel Kefurt, Jitka Moravcová, Milan Kodíček and Stanislav Forman



Synthesis and structure determination of some nonanomerically C–C-linked serine glycoconjugates structurally related to mannojirimycin

pp 2187–2195

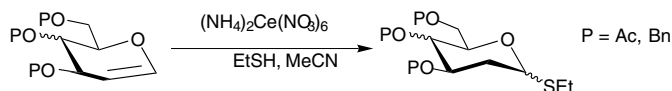
Júlia Mičová, Bohumil Steiner, Miroslav Kooš,* Vratislav Langer and Dalma Gyepesová



Catalytic ceric ammonium nitrate mediated synthesis of 2-deoxy-1-thioglycosides

pp 2197–2204

Somak Paul and Narayanaswamy Jayaraman*

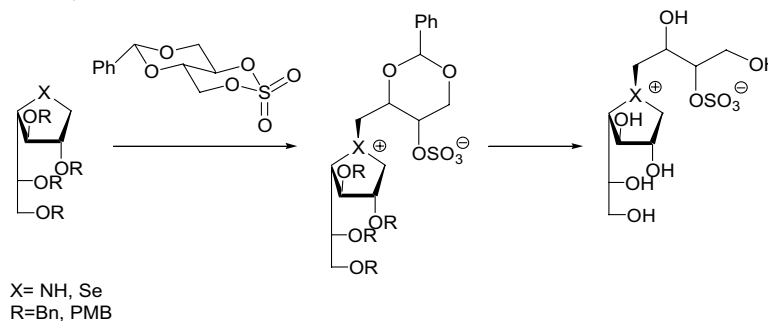


Synthesis of 2-deoxy-1-thioglycosides from glycals, mediated by catalytic amounts of ceric ammonium nitrate is reported. Glycosylation reactions of the thioglycosides with both aglycosyl and glycosyl acceptors afford α -anomeric glycosides exclusively.

Synthesis of novel ammonium and selenonium ions and their evaluation as inhibitors of UDP-galactopyranose mutase

pp 2205–2217

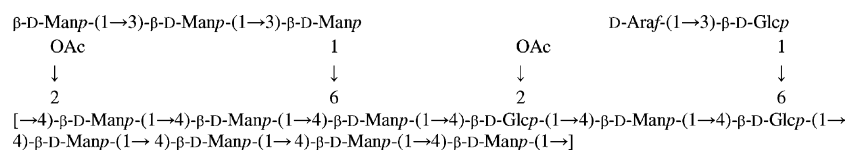
Natacha Veerapen, Yue Yuan, David A. R. Sanders and B. Mario Pinto*



Structural characterization of a 2-O-acetylglucomannan from *Dendrobium officinale* stem

pp 2219–2224

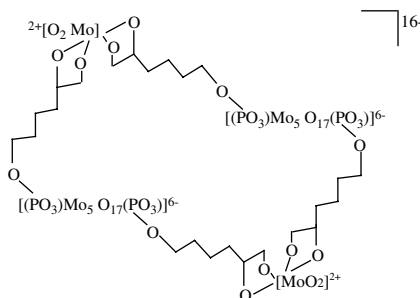
Yun-fen Hua, Ming Zhang, Cheng-xin Fu,* Zhang-hui Chen and Gilbert Yuk Sing Chan*



Multinuclear NMR study of the complexes of 6-phospho-D-gluconic acid with W(VI) and Mo(VI)

pp 2225–2232

M. Luísa Ramos* and Victor M. S. Gil

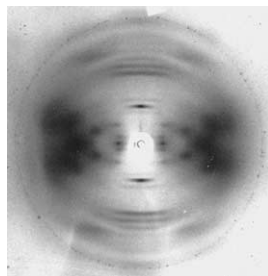


Three and six complexes have been identified with tungstate and molybdate, respectively, in aqueous solution, depending on pH and concentration; the structure of an important species formed with Mo(VI) is shown.

Synergistic interactions between the genetically modified bacterial polysaccharide P2 and carob or konjac mannan

pp 2233–2239

Michael Ridout, Paul Cairns, Geoffrey Brownsey* and Victor Morris

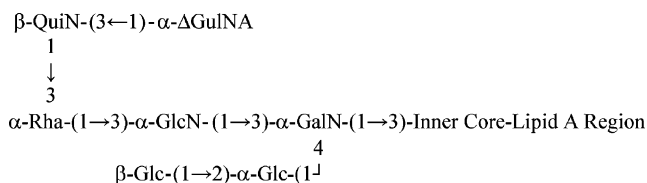


X-ray patterns of deacetylated polysaccharide P2 and glucomannan were used to investigate their synergistic interactions.

The structure of the phosphorylated carbohydrate backbone of the lipopolysaccharide of the phytopathogen bacterium *Pseudomonas tolaasii*

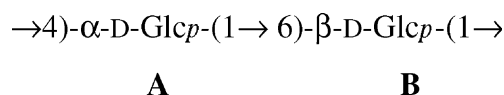
pp 2241–2248

Alba Silipo, Serena Leone, Antonio Molinaro,* Rosa Lanzetta and Michelangelo Parrilli

**Structural investigation of a water-soluble glucan from an edible mushroom, *Astraeus hygrometricus***

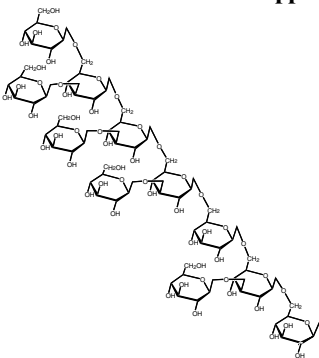
pp 2249–2254

Indranil Chakraborty, Soumitra Mondal, Malay Pramanik, Dilip Rout and Syed S. Islam*



Refinement of the structures of cell-wall glucans of *Schizosaccharomyces pombe* by chemical modification and NMR spectroscopy
Tomoko Sugawara, Seizo Takahashi, Masako Osumi and Naohito Ohno*

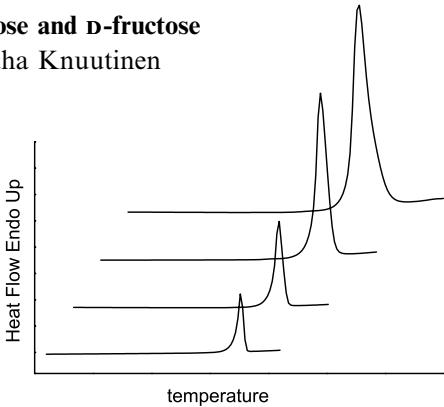
pp 2255–2265



The structure of the highly branched (1→6)-β-D-glucan of *S. pombe*.

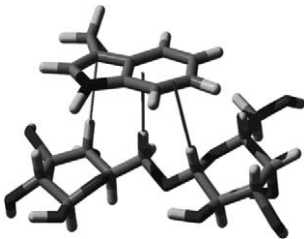
Melting behaviour of D-sucrose, D-glucose and D-fructose
Minna Hurta,* Ilkka Pitkänen and Juha Knuutinen

pp 2267–2273



Role of CH/π interactions in substrate binding by *Escherichia coli* β-galactosidase
Vojtěch Spiwok,* Petra Lipovová, Tereza Skálová, Eva Buchtelová, Jindřich Hašek and Blanka Králová

pp 2275–2280



Pectin methylesterases: sequence-structural features and phylogenetic relationships
Oskar Markovič and Štefan Janeček*

pp 2281–2295

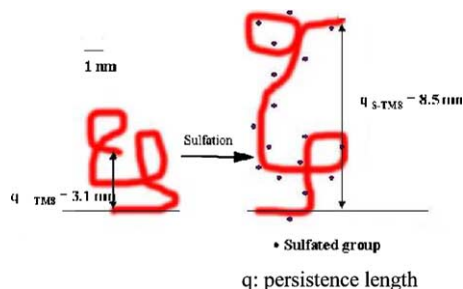
Clade	Enzyme	Region I	Region II	Region III	Region IV	Region V	C-term.
Plant 1	P83218_DAUCA	44_GVYREN	112_HQAVLR	134_YQDTLYV	157_DFIFG	223_LGRPWK	319
Plant 1a	O81415_ARATH39	257_GEYFEN	325_AQAVLR	347_YQDTLYV	370_DFIFG	436_LGRPWK	532
Plant 2	Q96576_LYCES3	268_GIYKEN	335_DQAVLR	357_YQDTLYA	380_DFIFG	446_LGRPWK	544
Plant 2a	Q42935_NICPL	41_GIYKEN	109_HQAVLR	131_FQDTLYT	154_DFIFG	220_LGRPWK	315
Plant 3	Q43867_ARATH65	316_GTYVEN	384_HQAVLR	406_FQDTLYP	429_DFIFG	490_LGRPWK	586
Plant 4	O80722_ARATH18	312_GLYREQ	380_HQAAIR	402_YQDTLYV	425_DFIFG	492_LGRPWK	586
Plant X1	Q96497_SILPR	105_GVYEET	174_HQAVLR	196_NQDTLYV	219_DFIFG	293_LGRPWK	379
Plant X2	Q9CAS7_ARATH9	77_GEYKEK	149_AQALSMR	171_FQDTLYD	194_DFIFG	244_LGRAMM	338
Fungi	Q12535_ASPAC	62_GTYDEQ	138_HQALALS	160_YQDTLLA	183_DFIFG	246_LGRPWS	331
Bacteria	P07863_ERWCH2	66_GVYNER	152_TQAVLY	177_YQDTLYV	199_DFIFG	265_LGRPWH	366

Conserved sequence segments of selected pectin methylesterases representing the individual clades. The three catalytic residues are highlighted in blue. Conserved Gly are highlighted in black. Cys, His, and Phe (Tyr) residues are highlighted in pink, turquoise, and yellow, respectively.

Evaluation of sulfated fungal β -glucans from the sclerotium of *Pleurotus tuber-regium* as a potential water-soluble anti-viral agent pp 2297–2301

Mei Zhang, Peter C. K. Cheung,* Vincent E. C. Ooi and Lina Zhang

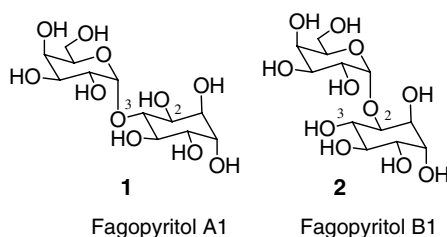
Introduction of sulfated groups in the native mushroom β -glucan (TM8) had enhanced anti-HSV activity that might be explained by the negative charge and extended conformation of the sulfated polysaccharide (STM8).



NOTES

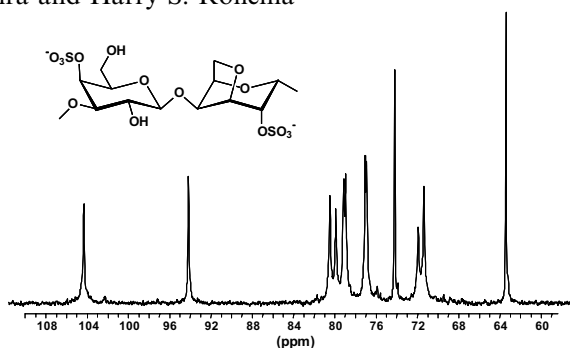
Synthesis of fagopyritols A1 and B1 from D-chiro-inositol pp 2303–2307

M. Belén Cid,* Francisco Alfonso and Manuel Martín-Lomas*



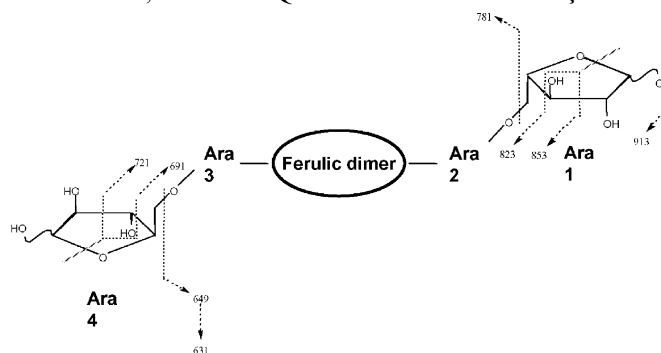
The revised NMR chemical shift data of carrageenans pp 2309–2313

Fred van de Velde,* Leonel Pereira and Harry S. Rollema



Isolation of diferulic bridges ester-linked to arabinan in sugar beet cell walls pp 2315–2319

Sébastien Levigne, Marie-Christine Ralet,* Bernard Quémener and Jean-François Thibault



Influence of alkali-freezing treatment on the solid state structure of chitin

pp 2321–2324

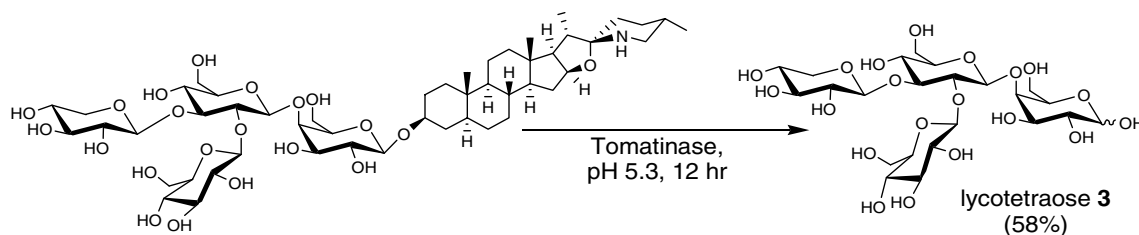
Fang Feng,* Yu Liu and Keao Hu

Crystallinity of chitin dramatically decreases within 3 days when soaked in frozen sodium hydroxide.

Enzymatic liberation of lycotetraose from the *Solanum* glycoalkaloid α -tomatine

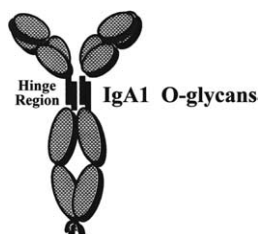
pp 2325–2328

Katherine Woods, Chris J. Hamilton* and Robert A. Field

**Human serum IgA1 is substituted with up to six O-glycans as shown by matrix assisted laser desorption ionisation time-of-flight mass spectrometry**

pp 2329–2335

Edward Tarelli,* Alice C. Smith, Bruce M. Hendry, Stephen J. Challacombe and Shideh Pouria



Human serum IgA1 is substituted with up to six O-glycans as shown by matrix assisted laser desorption ionisation time-of-flight mass spectrometry (MALDI-ToF-MS) analysis.

*Corresponding author

COVER

Well-defined glycoforms of glycoproteins can easily be obtained by oxidative coupling of synthetic thioaldoses with proteins that have a cysteine moiety in lieu of an asparagine residue carrying natural N-linked oligosaccharides. In vitro glycosylation offers several advantages such as quantitative conjugation, incorporation of oligosaccharides that display high bioactivities and the possibility of using convenient bacterial or yeast protein expression systems. The figure is related to Geert-Jan Boons' *Carbohydrate Research Award* paper, Carbohydr. Res., **2004**, 339, 181–193.



Full text of this journal is available, on-line from **ScienceDirect**. Visit www.sciencedirect.com for more information.



This journal is part of **ContentsDirect**, the *free* alerting service which sends tables of contents by e-mail for Elsevier books and journals. You can register for **ContentsDirect** online at: <http://contentsdirect.elsevier.com>

Indexed/Abstracted in: Chem. Abstr.; Curr. Contents: Phys., Chem. & Earth Sci. Life Sci. Current Awareness in Bio. Sci (CABS). Full texts are incorporated in CJELSEVIER, a file in the Chemical Journals Online database which is available on STN® International.



ISSN 0008-6215